



## Suaeda maritima MANGROVE LEAF EXTRACT ASSISTED BIOSYNTHESIS OF SILVER-COPPER OXIDE NANO COMPOSITE AND ITS PHOTOCATALYTIC APPLICATIONS

SURESH DODDA  
SUPRIYA GADI  
SWAPNA DUPPATI  
VENKATA CHALAPATHI RAO CHIPPADA  
PAUL DOUGLAS SANASI

Department of Engineering Chemistry, AU College of Engineering (A),  
Andhra University, Visakhapatnam - 530 003. AP



SURESH DODDA

### Introduction

Copper oxides nano particles have been found to be one of the most effective reagents for destroying a wide variety of bacterial and micro organismal pathogens which cause infections. A number of studies have been reported the use of copper oxide in combination with silver nano particles and also in a range of polymeric materials. Since nano silver has been proved as an effective antimicrobial activity at very low concentrations a number of products have been commercialized in the area of health care and in industry.

### Silver-copper oxide Nano Composites

"Copper oxide is a compound from two elements copper and oxygen which are block d and block p elements in periodic table respectively. In a crystal, copper ion is coordinated by four oxygen ions. Copper (Cu) and copper oxide (CuO) nanoparticles have attracted considerable attention because copper is one of the most important in modern technologies and is readily available [1]. There is increasing interest on copper nanoparticles due to their optical, catalytic, mechanical and electrical properties [2,3]. Copper oxide is

widely used in the field of catalysis, superconductors, ceramics and a kind of important inorganic materials. It can be used as a catalyst, catalyst support and electrode active material in the degradation of nitrous oxide with ammonia and oxidation of carbon monoxide [4]. Copper oxide nanoparticle is a powder soluble in dilute acid,  $\text{NH}_4\text{Cl}$ ,  $(\text{NH}_4)_2\text{CO}_3$ , potassium cyanide solutions and insoluble in water. It dissolves slowly in alcohols and ammonia solution. It can be reduced to metallic copper when meets hydrogen or carbon monoxide under high temperature.  $\text{CuO}$  nanoparticle can also be used as burning rate catalyst in rocket propellant. Nano copper oxide shows superior catalytic activity and selectivity than that of the common copper oxide powder. The particle size of nanometre copper oxide is between 1-100 nm. Compared with the ordinary copper oxide, nano  $\text{CuO}$  has peculiar physical and chemical properties such as surface effect, quantum size effect, volume effect and macroscopic quantum tunnelling effect in magnetic, optical absorption, chemical activity, thermal resistance and catalysis. Nano copper oxide attracts more and more people's attention and become one of the most extensively used inorganic materials" (Figure 1).

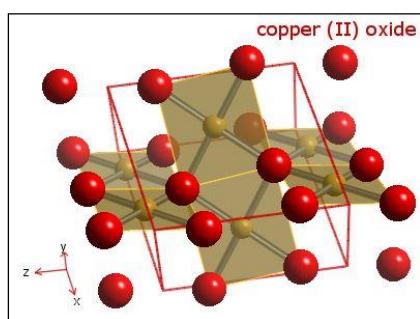


Figure 1: Structure of Copper Oxide

### 1.1 Copper Oxide Nano particles

A number of studies have been reported for the preparation of Copper oxide nanoparticles and their characterization. They have been formed with various irregular sizes ranging from few nano meters to micro meters

and shapes and various methods [5-20]. They have been used for the removal of methylene blue dye as adsorbent [5]. They have been used for various applications such as sensors, solar energy, storage devices, etc. [7]. They have been extensively used as catalysts various chemical transformations [8-12].

### Silver-Copper oxide Nano Composites

It has been reported in the literature that silver nanoparticles enhance the antibacterial activity of Copper oxide nano composites. The antibacterial activity of nano these composites found to be higher than the pure Copper oxide and Silver nano particles. This may be due to the surface interaction between bacteria cell walls and the nano composites. Cell wall damage is due to the penetration of nanoparticles and toxicity to the cells. Electrostatic interaction between nano composites and outer cell walls of the bacteria also causes death of the cell.

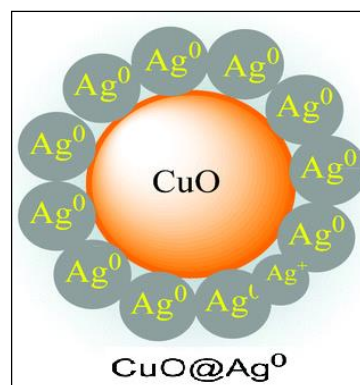


Figure 2 Representational Structure of Silver-copper oxide nanoparticles

In the present study, silver-copper oxide nano composites (Figure 2) with <25 nm diameters of silver particles via facile bio-hydrothermal method was reported. Silver nitrate and copper nitrate were the source materials and sodium hydroxide as the precipitating agent was used. Impact of leaf extract of *Suaeda maritima* - a mangrove associated from Korangi (Coringa) estuary, in Andhra Pradesh in India and incorporation of silver into copper oxide crystal on their

structural, optical, antibacterial behaviour, photocatalytic activity are studied in detail. The synthesized silver-copper oxide nano composites exhibit excellent antimicrobial activity against selected gram-negative and gram-positive bacteria and high photocatalytic activity under natural sunlight for the degradation of Congo red and Alizarin red dyes.

## 2 Materials and Methods

### 2.1 Preparation of *Suaeda maritima* leaf extract

*Suaeda maritima* leaves were collected, washed with double distilled water and dried for 15 days and then pulverized into fine powder using mechanical grinder. Then, 4 g of *Suaeda maritima* powder was mixed in 20 ml of double distilled water and stirred for 30 minutes at 60 °C. The leaf extract sample was cooled to room temperature and centrifuged for 10 minutes. The upper layer was filtered with filter paper. The 20% final extract of the leaf was used for the fabrication of Silver-copper oxide nano composites.

### 2.2 Methods

The synthesis of Silver-copper oxide nano composites with *Suaeda maritima* extract was prepared in single step bio-hydrothermal synthesis. General purpose autoclaves were applied for the preparation of Silver-copper oxide Nano composites (**Figure 3**). Copper nitrate (0.5 M), Silver nitrate (10 M) and sodium hydroxide (10 M) solution with different volumes were prepared and mixed under the stirring condition for 30 minutes, then *Suaeda maritima* leaf extract was added to above solutions and after that it was sonicated for 30 minutes. The sample was then shifted to the teflon liner and kept in an autoclaved vial in a hot air oven at 180 °C for 3 hours and oven cooled for 24 hours. Afterwards the sample was washed and dried and subjected for further characterization and analysis.



**Figure 3: Preparation of Silver-copper oxide nano composites**

## 3 Characterization

### 3.1 XRD Patterns of Silver-copper oxide Nano composite

X-ray diffraction (XRD) patterns of Silver-copper oxide nano composites were revealed by powder X-ray diffraction measurement. **Figure 4** illustrates the XRD pattern of silver-copper oxide nano composites contain copper oxide nano particles and silver nanoparticles.

**Figure 4** shows the XRD pattern of copper oxide nanoparticles. The sharp diffraction peaks in the XRD pattern distinctly depict the crystalline nature of the sample [21,22]. The standard diffraction peaks representing the crystal structure of copper oxide is hexagonal wurtzite structure according to the standard JCPDS data card. Diffraction peaks of other impurities were not detected. This proved that the peaks which were observed in the XRD spectrum belonged only to the Cu. The mean grain size of the Copper oxide nanoparticles was 16.78 nm. This was calculated from the three most intense peaks using Debye-Scherrer's formula [23,24]. The peaks in the XRD pattern show the face centered cubic (fcc) metallic structure of Ag (JCPDS card no. 04-0783) and hexagonal wurtzite structure of Copper oxide (JCPDS card no. 48-1548). For Silver nano

particles, the main characteristic peaks at  $2\theta$  values 37.2, 44.6 and 64.5, which belongs to the (111), (200), (220) planes of fcc, approving the formation of Silver because of the substitution of Silver<sup>+</sup> ions for Cu<sup>2+</sup> in the Copper oxide lattice. The XRD peaks for Silver-Copper oxide demonstrate the formation of clear, distinct phases for both Silver and Copper oxide. Formation of distinct phases for both Copper oxide and Silver reveals the synthesis of Silver-Copper oxide acrySTALLINE nanocomposite. The identified peaks represent the purity of nanocomposite.

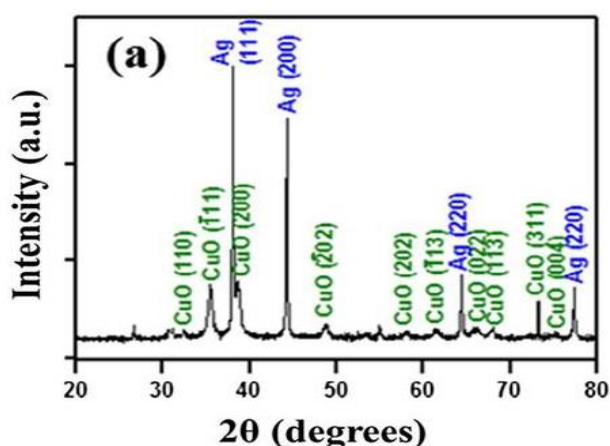


Figure 4 XRD Patterns of Silver-Copper oxide nano composite

### 3.2 FT-IR Analysis of Silver-Copper oxide Nano composite

The typical IR spectrum of Copper oxide nano particles, Silver-Copper oxide Nano composites and *Suaeda maritima* leaf extract are given in Figure 5. FTIR spectroscopy was used to identify the functional groups of the active components based on the peak value in the region of infrared radiation. The FTIR spectra of control leaf extract (before reaction without CuSO<sub>4</sub>) and synthesized Copper oxide nano particles (after reaction without CuSO<sub>4</sub>) are shown in Figure 5. The broad and strong peak at around 3440 cm<sup>-1</sup> can be attributed the O-H groups of alcohols and phenols. This peak shifted to lower field at 3393 cm<sup>-1</sup> in the synthesized Copper oxide nano particles. The band at 2850

cm<sup>-1</sup> is assigned to C-H stretching. The peaks observed in the range of 680-1454 cm<sup>-1</sup> have been assigned to alcohols and phenolic groups, C-N stretching vibrations of amines. The major peak observed to be 510 cm<sup>-1</sup> should be a stretching of Cu-O. The bands at 1630 cm<sup>-1</sup> of the leaf extract shifted to lower field at 1600 cm<sup>-1</sup>, in the product. The similar results have been reported in literature where Copper oxide nano particles was synthesized using different leaves extracts [25-27].

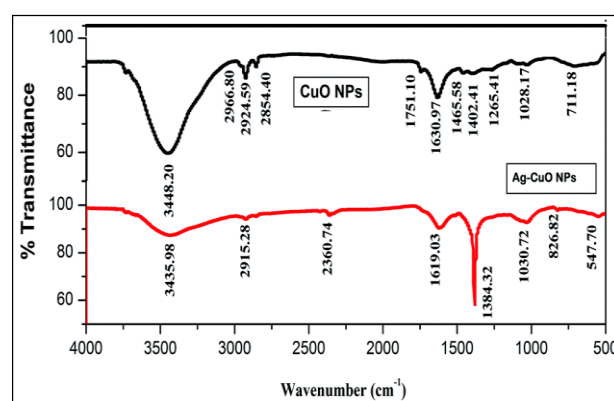
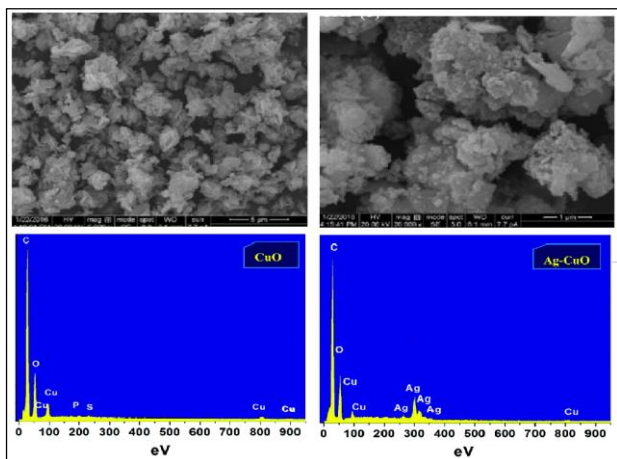


Figure 5 : FT-IR spectra of Copper oxide nano particles (Red) Silver-Copper oxide Nano composites (Black)

### 3.3 SEM and EDX Analysis of Silver-Copper oxide Nano composite

Figure 6 shows the SEM micrographs of the Silver-Copper oxide Nano composites. It shows the presence of spherical NPs with un-even grain size distribution. The Silver-Copper oxide Nano composites consist of a mesoporous morphology with a multiple porous network structure. The introduction of silver resulted in agglomeration of NPs. This is clearly evidenced by the formation of large spherical NPs surrounded by small NPs. From the afore mentioned discussions, it is therefore safe to conclude that the morphologies of as-prepared Copper oxide powders depends markedly on the concentration of the silver dopant.





**Figure 6 SEM and EDX images of Silver-Copper oxide nano composite**

It is clearly shown that in general the particles are roughly spherical and irregular shaped, which are free from agglomeration. It is observed that almost all of them are spherical in nature; further, the particles are agglomerated to form foam like bunch of particles. For Silver-Copper oxide nanoparticles, it is observed that there is more than one shape (spherical nanoparticles) as depicted in SEM image.

The composition and impurity contamination of the Silver-Copper oxide Nano composites was examined using energy dispersive X-ray (EDX) spectroscopy. **Figure 6** shows the EDX spectra of the Silver-Copper oxide sample. The presence of Cu, O and C in the EDX spectra confirms the successful pyrolysis of precursor to form Silver-Copper oxide Nano composites.

### 3.4 TEM Analysis of Silver-copper oxide Nano composite

**Figure 7** depicts the morphology and size of synthesized Silver-copper oxide nano composites using transmission electron microscopy (TEM). The TEM images display the formation of ~10 nm spherical Silver nano particles on the surface of Copper oxide particles. Nano composites were very obvious in TEM images. **Figure 7** illustrates the corresponding selected area electron diffraction

(SAED) pattern of Silver-Copper oxide Nano composites.

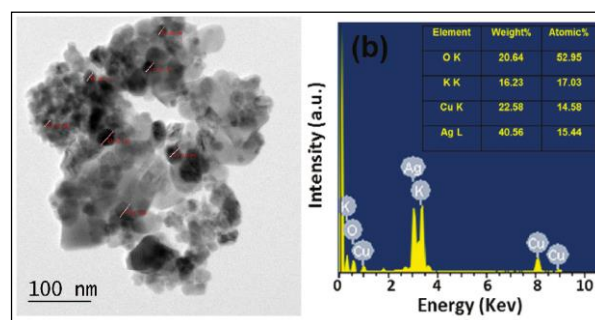


**Figure 7 : HR-TEM image of Silver-copper oxide nano composites**

The high resolution TEM result displays the fringes of 0.26 and 0.235 which are corresponding to [002] and [111] crystal planes of Copper oxide and Silver respectively. This is in agreement with SAED and XRD pattern. The crystalline nature of Copper oxide- Silver Nano composites was proved by the SAED pattern with the observation of bright spots. The appeared bright spots are attributed to (100), (102) and (101) planes of hexagonal structured Copper oxide while the mild spots are due to (111) and (200) planes of Silver crystal. **Figure 7** demonstrates the corresponding energy dispersive X-ray spectrometer (EDX) pattern. The result displays that there are no other impurities in EDX profile. The EDX findings visibly signify the presence of Cu, Silver and O in the synthesized Nano composites. The elemental analysis by EDX represents 3.73, 11.79 and 84.38 weight percentage of Nano composites for Ag, Cu and O respectively.

The TEM images show uniform dispersion of Silver-Copper oxide nanoparticles with average diameters of 20 nm, respectively. The average particle sizes determined by HR-TEM are closely matched to the crystallite size calculated by XRD and SEM analysis. This shows that the synthesized Copper oxide and Silver-Copper oxide nanoparticles are smaller in size and free from agglomeration. The TEM images clearly show that there is a layer of

nanoparticles, which are less than 20–25 nm on the surface.

### 3.5 Optical Absorption Studies of Silver-copper oxide

The optical absorption of Silver-copper oxide Nano composites at ambient temperature was evaluated using spectrophotometer. **Figure 8** shows the UV- visible spectroscopy of prepared Silver- Copper oxide Nano composites. The UV-Vis spectrum of Ag- Copper oxide Nano composites and nano Copper oxide displayed a maximum absorption peak at 381 and 350 nm respectively.

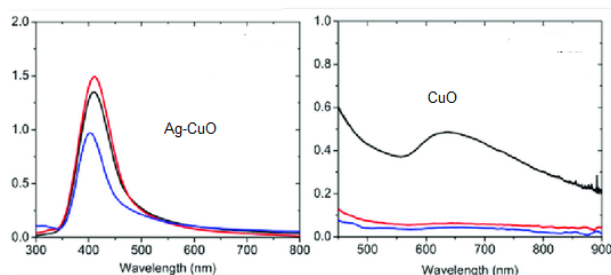


**Figure 8: UV-Visible spectrum of Silver-copper oxide and Copper oxide nano particles**

The band gap of bulk Copper oxide and Silver-copper oxide Nano composites was found to be 3.28 eV and 2.78 eV respectively. The presence of Silver nano particles improves the band gap absorption in comparison to the pure Copper oxide nano particles. Silver nano particles function in a range in between the conduction band (CB) and valence band (VB) of Copper oxide nano particles that accelerates the light absorption capacity.

## 4 Photocatalytic Degradation Studies of Congo Red and Alizarin Red dyes with Silver-copper oxide nano composites

### 1. Previous Studies on Photocatalytic Degradation of Congo Red dye

Azo dyes are a versatile class of colored organic compounds that have extensively been used in industry for applications such as textiles, paper, leathers, additives and analytical

chemistry [28]. During dye production and textile manufacturing processes, a large quantity of waste water containing dyestuffs with intensive color and toxicity are introduced into the aquatic systems [29]. In such cases, removing color from wastes is imperative, because the presence of even small amounts of dyes (below 1 ppm) is clearly visible and influences water environment considerably.

Congo Red dye (sodium salt of benzidine diazo-bis-1-naphthyl amine-4-sulphonic acid) is one of the important secondary azodye which is used for dyeing cotton in textile industry and also in paper and wood pulp industries. Various photocatalysts have been reported in the literature for the photocatalytic degradation of Congo Red dye such as Chitosan modified PVC-Copper oxide composites [30], ZnO-CdS core shell nano structure [31], Nano cobalt ferrite thin film [32], ZnO [33], SPIONs, ZnO and Ce-TiO<sub>2</sub> [34], Charcoal and Gram husk [35], ZnO-ZnFe<sub>2</sub>O<sub>4</sub> nano composites [36], Fe<sup>3+</sup>/C/S doped TiO<sub>2</sub> [37], TiO<sub>2</sub> [38] and many other materials.

### Previous Studies on Photocatalytic Degradation of Alizarin Red dye

Alizarin Red S (1,2-dihydroxy-9,10-anthraquinonesulfonic acid sodium salt, ARS, Alias Mordant Red 3, C.I. no. 58005,) is a watersoluble, widely used anthraquinone dye. It is synthesized by sulfonation of alizarin which is a natural dye obtained from madder (*Rubia tinctorum*, *L. Rubiaceae*). In clinical practices, it is also used to stain synovial fluid to assess for basic calcium phosphate crystals. Anthraquinone dyes like ARS are durable pollutants, released especially by textile industries in the aquatic ecosystems. Removal of these from industrial wastewaters is a crucial process, from both economical and environmental points of view.

The Alizarin Red-S dye was used in this experiment procured from BDH India Ltd. (Molecular Formula C<sub>14</sub>H<sub>18</sub>O<sub>7</sub>NaS, M.Wt. = 240.21, C.I. No. 58005, λ<sub>max</sub>= 430nm). The

stock solution was prepared by dissolving 0.1g/L of dye in water and made up a stock solution in volumetric flask. By making 20, 40, 60 ppm solution. The concentration of the dye solution was determined spectrophotometrically. The structure of Alizarin Red-S is given in **Figure 2**.

Various photocatalysts have been reported in the literature for the photocatalytic degradation of Alizarin Red S dye such as Alumina [39], ZnO& TiO<sub>2</sub> [40], nano strantium titanate [41], TiO<sub>2</sub>-UV System [42], Bi<sub>2</sub>MTaO<sub>7</sub> (M = Al, Fe, Ga, In) [43], Ozonation [44], Fe-Co Nanoparticles [45], ZnO-CdO nano material [46], Ni doped WO [47], Nano strantium titanate [48], Bi<sub>2</sub>MTaO<sub>7</sub> (M = Al, Fe, Ga, In) [47], Fe<sub>2</sub>O<sub>3</sub>/NiS [49]

It is necessary to develop and improve effective methods of wastewater treatment in order to remove color from effluents. Physical and chemical techniques such as coagulation, adsorption on activated carbon, ultra filtration and reverse osmosis are generally used efficiently to remove dyes from textile wastewater. However, these processes are considered as nondestructive since they merely transfer the dye from liquid to solid wastes. Consequently, the regeneration of the adsorbent material and post-treatment of solid wastes, which are expensive operations, are needed [50, 51]. Advanced oxidation processes (AOPs) are alternative techniques of destruction of dyes and many other organics in wastewater and effluents. These processes generally involve UV/H<sub>2</sub>O<sub>2</sub>, UV/O<sub>3</sub> or UV/Fenton's reagent for the oxidative degradation of contaminants [52].

Among the various AOPs, semiconductor-mediated photocatalysis has been given great credit over the past few years due to its potential to destroy a wide range of organic and inorganic pollutants at ambient temperatures and pressures, with no harmful by-products [53].

In order to achieve a more effective photocatalytic degradation, it is necessary to consider the surface charge property of semiconductors and nature of dye molecules. pH affects the surface charge of semiconductors and can also lead to aggregation phenomenon in dye solutions. Aggregation is one of the features of dyes in solution and ionic dyes tend to aggregate in diluted solutions, leading to dimer formation and sometimes even higher order aggregates.

In the present work, visible light induced photocatalytic degradation of Congo Red and Alizarin Red dyes in aqueous medium was investigated by employing Silver-copper oxide bimetallic nanoparticles. The efficiency of the composites towards the photocatalytic degradation of Congo Red and Alizarin Red dyes was assessed by analyzing the effect of Silver-copper oxide bimetallic nanocomposites with increase in the content of silver and effect of pH of the dye solution. Photocatalytic degradation of Congo Red and Alizarin Red dyes was enhanced by contriving the composites into visible light absorption on dispersing silver on the surface of Copper oxide nanoparticles. With an optimum increase in the silver content, the photocatalytic activity of the composites was improved and a superior photocatalytic activity was observed with 10% silver-copper oxide bimetallic nanocomposite material.

## 2 Photocatalytic studies

The photocatalytic activity of the synthesized nanocomposite materials was examined for the visible light degradation of Congo red and Alizarin red dye solutions. 10 mg of the each composite material was dispersed separately in six different sets of 100 ppm concentrated dye solutions and kept under magnetic stirring in dark for 30 minutes to establish desorption/adsorption equilibrium. Then the mixtures were kept under visible lamp and 5 mL of aliquots were collected for every 15 minutes of time interval. These aliquots were analyzed by using UV-Vis

spectrophotometer. **Figure 9** shows the decrease in absorbance of the dye solution in the presence of nano copper oxide and the composite materials. It was clear that the absorbance was gradually decreased with increase in mole % of Silver-copper oxide in the composites. It was also clear that the irradiation time was reduced from 180 minutes to 60 minutes by 10 mole % silver-copper oxide bimetallic nano particle material for the Congo Red and Alizarin Red dyes. This may be attributed to the significant change in the band gap (2.85 eV) of the material compared to nanocopper oxide (3.2 eV). On comparison with this material, almost similar degradation was observed with 20 mole % silver copper oxide nanocomposite material as its band gap was around 2.89 eV.

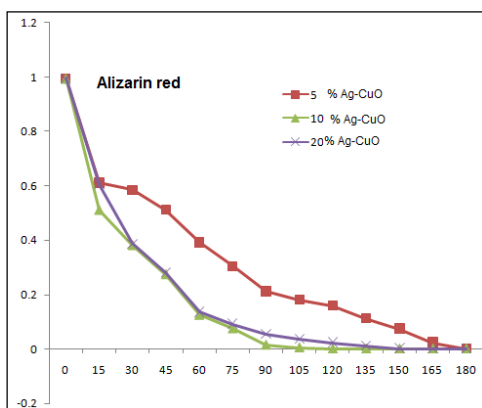
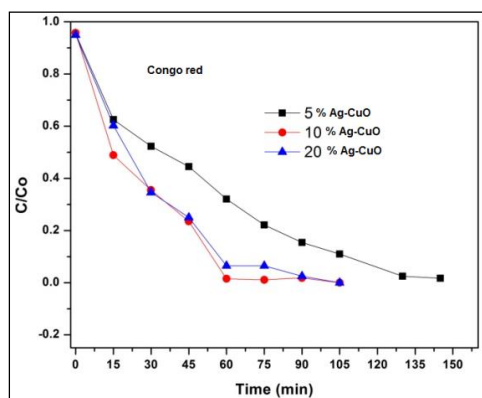


**Figure 9** Photocatalytic degradation of Congo Red and Alizarin Red dyes dye in the presence of x mole % silver copper oxide nano composites under visible light irradiation.

[Dye]= 10 ppm, Catalyst load = 10 mg/ 100 mL

### 3 Effect of mole % of silver on photocatalytic degradation:

The photocatalytic degradation of Congo Red and Alizarin Red dyes has been carried out with x% silver copper oxide nano composites under visible light. **Figure 10** shows the efficiency of mole % of silver in the composites for degradation of the dye. It has been clearly observed that the % of degradation of the dye solution was enhanced with increased of silver content in the composites from 5 % to 20 % and a superior degradation efficiency (100 %) was achieved with 10 mole % silver copper oxide composite material. This can be attributed to high capability of nitrogen and sulphur dopants in the lattice sites of copper oxide which can store electrons and shuttle the electrons. The presence of Silver atoms in the form of nano silver also controls the rapid recombination of  $e^-/h^+$  pairs in the nano copper oxide particles and thus provides a medium for the photochemical oxidation of the organic dyes [54]. Further increase in the mole % of silver in the composite did not show any appreciable change in the degradation efficiency. This may be due to agglomeration of the silver particles to form large particles, thereby decreasing the specific surface areas of the nano copper oxide composites [55].

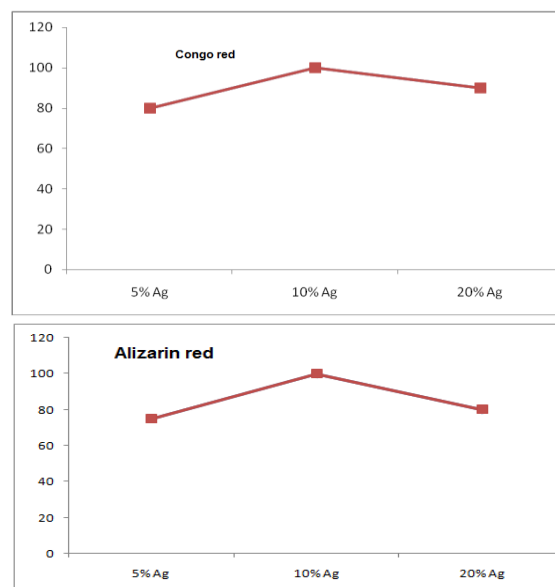


**Figure 10** Effect of mole % of silver on copper oxide nano composites in % degradation of



Congo Red and Alizarin Red dyes From the graph, for 5, 10, 20 % silver copper oxide nanocomposites respectively, Catalyst load= 10 mg/ 100 mL

#### 4 Effect of amount of photo catalysts dosage

A number of reports have demonstrated that catalyst dosage has a large influence on the reaction rate. The effect of photocatalysts (10% silver nano copper oxide composite) dosage on the photocatalytic degradation of Congo Red and Alizarin Red dyes was studied and shown in **Figure 11**. The dosage amount was varied from 0.1 g to 1 g/ L and all the observations are carried out at room temperature. It can be concluded that, increasing the catalyst dosage from 0.1 g to 0.5 g/ L, the degradation efficiencies were significantly improved and the values are presented in **Figure 11**. This phenomena may be due to increase in the amount of catalysts dosage, which would increase the reactive sites that can correspondingly produce more reactive oxidative species. However, too much catalyst dispersed in the system will possibly increase light scattering and decrease light penetration [76], resulting in the reduction of degradation efficiency of Congo Red and Alizarin Red dyes in a system with excessive photocatalysts. 0.1 g 10% silver-copper oxide bimetallic nano particle performs the best in removing the organic pollutants in wastewater under visible light irradiation. So the experiment was carried out with 0.1 g/L nano composite.

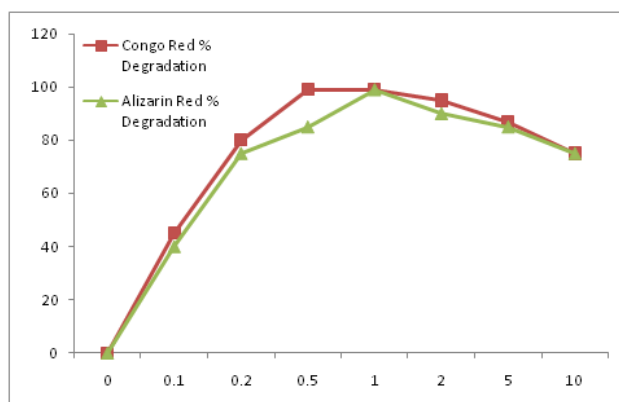


Figure 11 Effect of catalyst loading on the % degradation of Congo Red and Alizarin Red dyes, for 5, 10, 20 % silver copper oxide nanocomposites respectively, Catalyst load= 10 mg/ 100 mL

#### 5 Effect of amount of H<sub>2</sub>O<sub>2</sub>

The effect of the initial H<sub>2</sub>O<sub>2</sub> dosage on the decomposition efficiency of Congo Red and Alizarin Red dyes is shown in **Figure 12**. The oxidation degradation conversion of Congo Red and Alizarin Red dyes increased with the amount of H<sub>2</sub>O<sub>2</sub> and reached a maximum when the amount of H<sub>2</sub>O<sub>2</sub> added was 1.0 mL. After that, the decolorization efficiency drastically decreased, as the amount of H<sub>2</sub>O<sub>2</sub> was further increased which is represented in **Figure 12**. When the amount of H<sub>2</sub>O<sub>2</sub> was first increased, more reactive radicals were generated on the surface of silver-copper oxide composite. At a low concentration, H<sub>2</sub>O<sub>2</sub> inhibits the recombination of photogenerated electrons and holes. However, at a high concentration, H<sub>2</sub>O<sub>2</sub> is a powerful OH· scavenger, which would decrease the oxidation activity. Therefore, it is necessary to choose a proper amount of H<sub>2</sub>O<sub>2</sub> according to the kinds and concentrations of pollutants in order to optimize the oxidation efficiency of H<sub>2</sub>O<sub>2</sub>.

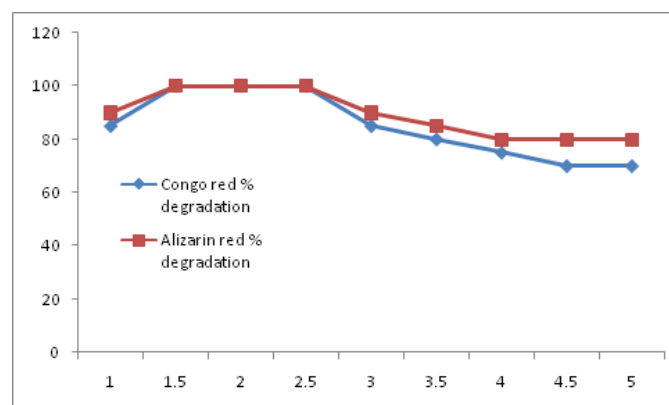
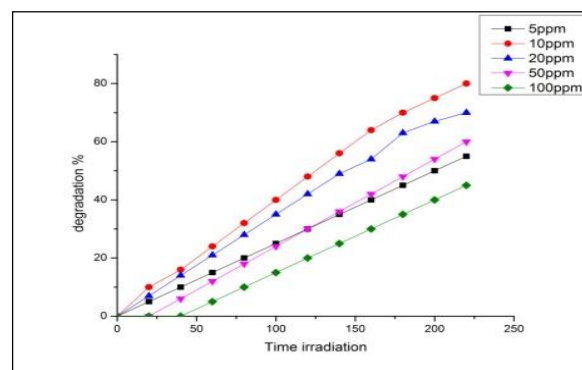


Figure 12 Effect of amount of H<sub>2</sub>O<sub>2</sub>

#### 6 Effect of Initial Dye Concentration

The effect of initial dye concentration of Congo Red and Alizarin Red dye solutions on the photocatalytic degradation is an important aspect of the study. The effect of this parameter

on the degree of photodegradation was studied by varying the initial concentration over a range of 0.1mg to 0.5mg/ L. As the concentration of the dye is increased, the rate of dye degradation is decreased, indicating that to either increase the catalyst dose or time span for the complete removal. **Figure 13** depicts the time dependent graphs of the degradation of Congo Red and Alizarin Red dyes at different concentrations. The possible explanation for this behaviour is that as the initial concentration of the dye increases, the solution becomes more intense coloured and the path length of photons entering the solution decreases. It means that only fewer photons are reached on the surface of the catalyst. The same effect was during the photocatalytic degradation of Alizarin Red dye with Copper oxide catalyst. This suggests that as the initial concentration of the dye increases, the requirement of catalyst surface needed for the degradation also increases. Since illumination time and amount of catalyst are constant, the OH radical (primary oxidant) formed on the surface of Copper oxide is also constant. So the relative number of free radicals attacking the dye molecules decreases with increasing amount of the catalyst. Hence, at higher concentration, degradation decreases at sufficiently longer distances from the light source or reaction zone due to the retardation of penetration of light. Thus, the rate of degradation decreases with increase in concentration of dyes. It has been observed from the **Figure 13** that increasing concentration of dye solution from 10 to 100 ppm decreases the percentage degradation rate and it was found that at 10 ppm dye concentration, degradation was 80% and at 50 ppm dye concentration, percentage degradation was reduced to 60% [16].



**Figure 13** Effect of Initial Dye Concentration

### 7 Effect of pH on degradation of dye solution

The effect of pH of the dye solution in photocatalytic degradation was studied with 10 mole % silver copper oxide nanocomposites material by varying the concentrations of HCl and NaOH solution and was shown in **Figure 14**. These effects were studied by varying the pH of the dye solution from 5.0-12.0. A steady increase of photocatalytic degradation was observed from pH 5.0-7.0 and reached maximum degradation effect in the pH range of 8.0-9.0. However, the degradation efficiency slowly decreased from pH 10 and it clearly shows the dye solution has maximum degradation in the pH range of 8.0-9.0. The pH affects the surface properties of the catalysts and also dissociates the dye molecules by formation of hydroxyl radicals. This can be due to agglomeration of the nano copper oxide particles at low pH which makes the degradation efficiency less. At low pH conditions, the azo groups in Congo Red and Alizarin Red dyes (-N=N-) are susceptible to electrophilic attack and the high concentration of H<sup>+</sup> ions decreases the electron densities in the azo group [22].

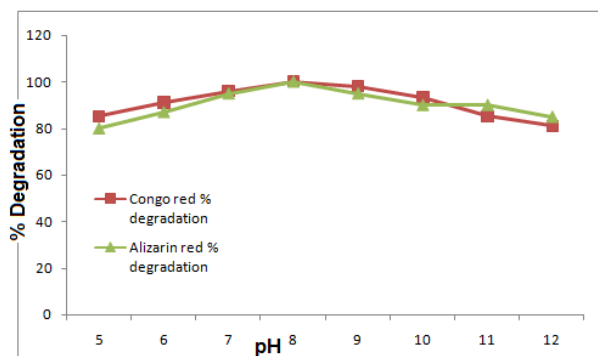


**Figure 14** Effect of pH on the degradation of the dye with 10 mg of 10% silver-copper oxide nanocomposite material [Dye]= 10 ppm

### 8 Effect of Temperature

Temperature of the photocatalytic reacting system was also varied from 0 to 80°C to explore its effect on the photocatalytic performances of the prepared samples under visible light irradiation. When the temperature of the reacting system is in the range of 20–60 °C, the photocatalytic performances in degrading Congo red and Alizarin Red dyes were similar, and only slight increases were found with the increase in temperature. However, when the temperature was fixed at 0 °C, the photocatalytic activity was significantly reduced. This might be because the mass transfer of pollutants to the surface of photocatalysts was decreased and the generation rate of oxidative species was also reduced. When the temperature was as high as 80 °C, the photocatalytic activity was greatly decreased. High temperature favours the recombination of charge carriers and desorption of adsorbed organics on the photocatalysts. The results (**Figure 15**) can be regarded as evidence of temperature controller needed for solar devices.

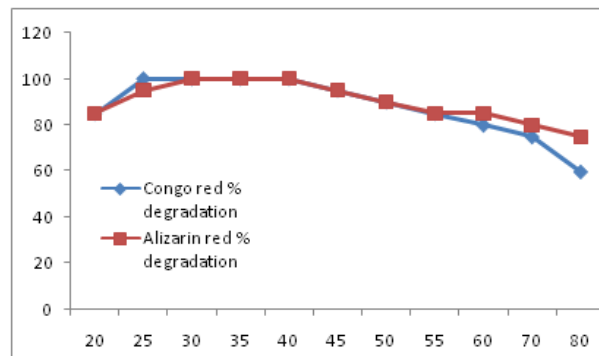


**Figure 15** Effect of Temperature on the photodegradation of Congo Red and Alizarin Red dyes with Silver Copper oxide composite

### 9 Reusability of the Catalyst

Reusability of the silver copper oxide composite catalyst was also studied under the optimized conditions. After the reaction is finished, the catalyst was recovered and washed with distilled water and ethyl alcohol. The recovered catalyst was treated again by H<sub>2</sub>O<sub>2</sub> for the next degradation run. The removal efficiency of Congo Red and Alizarin Red dyes was 90% in the first run, 60% in second run and 28% in the third run over 80-150 min in under visible light irradiation which is shown in **Figure 16** The decrease can be attributed to the loss of photocatalysts between two runs and some refractory intermediates adsorbed on their surface which are difficult to be destroyed. Despite this slight reduction in removal efficiency, the stability of the reused silver-copper oxide bimetallic nano particle photocatalyst after degradation of Congo Red and Alizarin Red dyes is still significant.

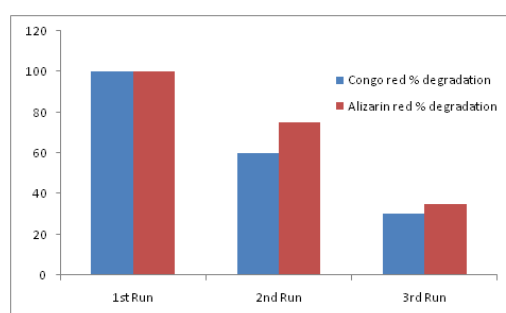


**Figure 16:** Reusability capacity of Silver-copper oxide Nano composite

## 5 Plausible mechanism of photocatalytic degradation

The schematic illustration of the visible light induced photocatalytic degradation of Congo Red and Alizarin Red dyes dye in the presence of silver-copper oxide composites was shown in **Figure 17**. On visible light irradiation, the electrons ( $e^-$ ) present in the valence band (VB) of the nano copper oxide particles gets excited to the conduction band (CB). This stage is referred to as the semiconductor's photo-excitation stage creating a negative-electron ( $e^-$ ) and positive-hole ( $h^+$ ) pair. In the absence of GO, these  $e^-/h^+$  pairs combine vigorously and results in a very low photoactivity. On doping with Silver atoms present in silver, this  $e^-/h^+$  recombination can be arrested and shifts the electrons for the photocatalytic degradation [23]. This negative electron subsequently transfers to the surface of the composite material to react with water and oxygen and yields hydroxyl radicals and super oxide ions respectively. These hydroxyl radicals and super oxide ions would oxidize the Congo Red and Alizarin Red dyes.

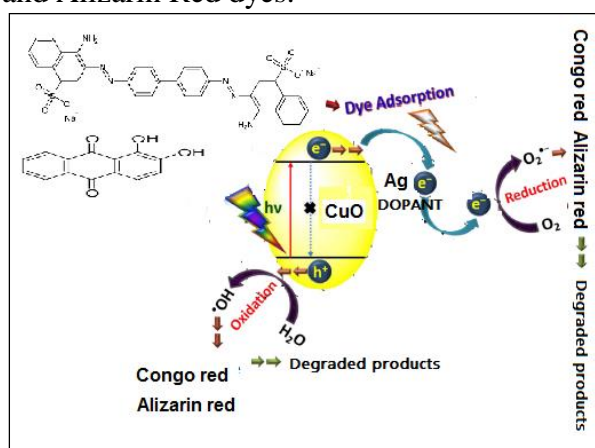


**Figure 17** Photocatalytic degradation of Congo Red and Alizarin Red dyes dye in the presence of x mole % silver copper oxide nanocomposites under visible light irradiation

## 6 Applications

The present study is applicable in the photocatalytic degradation of many other organic dyes like Rhodamine B, Alizarin Red

S, Eriochrome black-T etc under visible light irradiation. Further, maximum degradation may be achieved with a low dosage of the x mole % silver copper oxide nanocomposites.

## 7 Conclusions

A one step *Suaeda maritima* mangrove leaf extract biosynthesis of silver-copper oxide nano composites has been prepared. The as-prepared nano composite materials were characterized by XRD, FESEM, and UV-Vis DRS techniques and their efficiency was analyzed for photocatalytic degradation of Congo Red and Alizarin Red dyes under visible light irradiation. It was observed that in 60 minutes, 100 % of the dye solution was degraded with 10 mole % silver-copper oxide bimetallic nano particle material for 10 mg dosage of catalyst and 100 ppm dye concentration.

## 8 References

- [1] Guajardo-Pacheco MJ; Morales-Sanchez JE; González-Hernández J; Ruiz F, Synthesis of copper nanoparticles using soybeans as a chelant agent. *Mater Lett*, **2010**, 64, 1361-1364.
- [2] Xi Y; Hu C; Gao P; Yang R; He X. et al., Morphology and phase selective synthesis of  $Cu_xO$  ( $x = 1, 2$ ) nanostructures and their catalytic degradation activity, *Bioelectron Nanotechnol J*, 1(1), *Mater Sci Eng B*, **2016**, 166, 113-117.
- [3] He Y, A novel solid-stabilized emulsion approach to  $CuO$  nanostructures microspheres. *Mater Res Bull*, **2007**, 42, 190-195.
- [4] Motogoshi R; Oku T; Suzuki A; Kikuchi K; Kikuchi S, et al. Fabrication and characterization of cuprous oxide: fullerene solar cells. *Synth Met*, **2010**, 160, 1219-1222.
- [5] Mustafa G; Tahir H; Sultan M; Akhtar N, Synthesis and characterization of cupric oxide ( $CuO$ ) nanoparticles and their application for the removal of dyes, *African*



- Journal of Biotechnology*, 2013, 12, 6650-6660.
- [6] Suleiman M; Mousa M; Hussein A; Hammouti B; Hadda T B, et al. Copper(II)-Oxide nanostructures: synthesis, characterizations and their applications-review. *J Mater Environ Sci*, **2013**, 4, 792-797.
- [7] Aparna Y; Rao K V; Subbarao P S, Synthesis and characterization of cuo nano particles by novel sol-gel method. *IPCBE*, **2012**, 48, 156-160.
- [8] Abboud Y; Saffaj T; Chagraoui A; Bouari A E; Brouzi K, et al. Biosynthesis, characterization and antimicrobial activity of copper oxide nanoparticles (CONPs) produced using brown alga extract (*Bifurcaria bifurcata*). *Appl Nanosci*, **2014**, 4, 571-576.
- [9] Lanje A S; Sharma S J; Pode R B; Ningthoujam R S, Synthesis and optical characterization of copper oxide nanoparticles. *Adv Appl Sci Res*, **2010**, 1, 36-40.
- [10] Volanti DP; Keyson D; Cavalcante LS; Simões AZ; Joya MR, Longo E; Varela JA; Pizani PS; Souza AG, Synthesis and characterization of CuO flower-nanostructure processing by a domestic hydrothermal microwave. *J Alloys Comp*, **2008**, 459, 537 - 542.
- [11] Sahay R.; Sundaramurthy J; Kumar P S; Thavasi V; Mhaisalkar S G, Synthesis and characterization of CuO nanofibers, and investigation for its suitability as blocking layer in ZnO NPs based dye sensitized solar cell and as photocatalyst in organic dye degradation. *J Solid State Chem.*, **2012**, 186, 261-267.
- [12] Wongpisutpaisan N; Charoonsuk P; Vittayakorn N; Pecharapa W, Sonochemical synthesis and characterization of copper oxide nanoparticles. *Energy Procedia*, **2011**, 9, 404-409.
- [13] Ghane M; Sadeghi B; Jafari A R; Pakenjhad A R, Synthesis and characterization of a Bi-Oxide nanoparticle ZnO/CuO by thermal decomposition of oxalate precursor method. *Int J Nano Dim*, **2010**, 1, 33-40.
- [14] Ethiraj A; Kang D J, Synthesis and characterization of CuO nanowires by a simple wet chemical method. *Nanoscale Res Lett*, **2012**, 7, 70.
- [15] Mousa M K, Wastewater disinfection by synthesized copper oxide nanoparticles stabilized with surfactant. *J Mater Environ Sci*, **2015**, 6, 1924-1937.
- [16] Nasibulin A G; Ahonen P P; Richard O; Kauppinen E I; Altman I S, Copper and copper oxide nanoparticle formation by chemical vapor nucleation from copper (II) acetylacetonate. *J Nanopart Res*, **2001**, 3, 383-498.
- [17] Zhu H; Han D; Meng Z; Wu D; Zhang C, Preparation and thermal conductivity of CuO nanofluid via a wet chemical method. *Nanoscale Res Lett*, **2011**, 6, 181.
- [18] Kannaki K; Ramesh P S; Geetha D, Hydrothermal synthesis of CuO nanostructure and their characterizations. *Int J Sci Eng Res*, **2012**, 3, 1-4.
- [19] Darezereshki E; Bakhtiari F, A novel technique to synthesis of tenorite (CuO) nanoparticles from low concentration CuSO<sub>4</sub> solution. *J Min Metall B Metall*, **2011**, 47, 73-78.
- [20] Srivastava S; Kumar M; Agrawal A; Dwivedi S K, Synthesis and characterisation of copper oxide nanoparticles. *IOSR J Appl Phys*, **2013**, 5, 61-65.
- [21] Ren G; Hu D; Cheng EW; Vargas-Reus MA; Reip P; Allaker RP, Characterization of copper oxide nano particles for antimicrobial applications. *Int J Antimicrob Agents* **2009**, 33(6), 587-590.

- [22] Sankar R; Manikandan P; Malarvizhi V; Fathima T; Shivashangari KS; Ravikumar V, Green synthesis of colloidal copper oxide nanoparticles using Carica papaya and its application in photocatalytic dye degradation. *Spectrochim Acta Mol Biomol Spectrosc* **2014**, 121, 746-750.
- [23] Yallappa S; Manjanna J; Sindhe MA; Satyanarayan ND; Pramod SN; Nagaraja K, Microwave assisted rapid synthesis and biological evaluation of stable copper nanoparticles using T. arjuna bark extract. *Spectrochim Acta Mol Biomol Spectrosc* **2013**, 110, 108-115.
- [24] Kwak K; Chongyoun K, Viscosity and thermal conductivity of copper oxide nanofluid dispersed in ethylene glycol. *Korea-Aust Rheol j* **2005**, 17(2), 35-40.
- [25] Jafarirad S; Mehrabi M; Pur ER, Biological Synthesis of Zinc Oxide and Copper Oxide Nanoparticles. International Conference on Chemistry, *Biomedical and Environment Engineering*. **2014**, 62-64.
- [26] Sankar R; Manikandan P; Malarvizhi V; Fathima T; Shivashangari KS; Ravikumar V, Green synthesis of colloidal copper oxide nanoparticles using Carica papaya and its application in photocatalytic dye degradation. *Spectrochimica Acta A: Molecular and Biomolecular Spectroscopy*. **2014**, 121, 746-750.
- [27] Awwad AM, Albiss BA; Salem NM, Antibacterial Activity of synthesized Copper Oxide Nanoparticles using Malva sylvestris Leaf Extract. *SMU Medical Journal*, **2015**, 2(1), 91-101.
- [28] Dakiky M, Nemcova I, *Dyes Pigments*, **2000**, 44, 181.
- [29] Brown MA; De Vito SC; Rev C, *Environ. Sci. Technol.* **1993**, 23, 249.
- [30] Linda T; Muthupoongodi ; Sahaya Shajan X; Balakumar S, Effect Of Chitosan On Photocatalytic Degradation Of Congo Red Dye Using PVC/TiO<sub>2</sub>Nano Composites Under UV-Light Irradiation, *International Journal of Chem. Tech Research* , **2014**, 6(13), 5378 – 5381. CODEN (USA): IICRGG ISSN : 0974
- [31] Mohammad Hossein Habibi; Mohammad Hossein Rahmati, *Spectrochimica Acta Part A: Molecular and Biomolecular Spectroscopy* The effect of operational parameters on the photocatalytic degradation of Congo Red organic dye using ZnO–CdS core–shell nano-structure coated on glass by Doctor Blade method, **2015**, 137, 160-164
- [32] Manohar RP; Annapurna Jha, Synthesis of Magnetic Nano Sized Cobalt Ferrite Thin Film by Chemical Bath Deposition Method and their Photocatalytic Application for Removal of Congo Red Dye, *Journal of Applicable Chemistry*, **2018**, 7 (4), 779-784
- [33] Movahedi AR; Mahjoub S; Janitabar-D, Photodegradation of Congo Red in Aqueous Solution on ZnO as an Alternative Catalyst to TiO<sub>2</sub> M. *J. Iran. Chem. Soc.*, 2009, 6(3). 570-577
- [34] Preethi MEL; Prithika S; Yamini R, Solar Light Aided Photobleaching of Congo Red Dye Using Spions: a Novel Route for Complete Dye Degradation, *International Journal of Innovative Research in Science, Engineering and Technology*, 2015, 4.
- [35] Jain R; Sikarwar S, Photocatalytic and adsorption studies on the removal of dye Congo Red from waste water, *Int. J. Environment and Pollution*, **2006**, 27, 158–178.
- [36] Rahmayeni A; Ramadani Y; Stiadi N; Jamarun ES, Photocatalytic Performance of ZnO-ZnFe<sub>2</sub>O<sub>4</sub> Magnetic Nanocomposites on Degradation of Congo Red Dye under Solar Light Irradiation *Arief Journal of Materials and Environmental Sciences*, **2017** 8(5), 1634-1643
- [37] William Wilson A; Samuel Osei-Bonsu O; Sudheesh Kumar S; Poomani P, Govender Comparative Photocatalytic Degradation of

- Monoazo and Diazo Dyes Under Simulated Visible Light Using Fe<sup>3+</sup>/C/S doped-TiO<sub>2</sub> Nanoparticles *Acta Chim. Slov.* **2016**, 63, 380–391.
- [38] Harun H; Rahman MNA; Kamarudin WFW; Irwan Z; Muhammad A; Akhir NEFM, Yaafar MR, Photocatalytic Degradation Of Congo Red Dye Based Ontitanium Dioxide Using Solar And UV Lamp N. *J Fundam Appl Sci.* **2018**, 10(15), 832-846
- [39] Rehman R; Mahmu T; Anwar Jamil; Salman Md.; Umer Shafique; Waheed-Uz-Zaman; Furqan Ali, Removal of Alizarin Red S (Dye) from Aqueous Media by using Alumina as an Adsorbent, *J.Chem.Soc.* **2011**, 33, 2.
- [40] Joshi KM; Shrivastava VS. Degradation of Alizarine Red-S (A Textiles Dye) by Photocatalysis using ZnO and TiO<sub>2</sub> as Photocatalyst *International Journal Of Environmental Sciences*, **2011**, 2, 1.
- [41] Loghman AK; Salar Zohoori ; Mohammad Esmail Yazdanshenas, Photocatalytic degradation of azo dyes in aqueous solutions under UV irradiation using nano-strontium titanate as the nanophotocatalyst, *Journal of Saudi Chemical Society*, **2014**, 18, 581–588
- [42] Šima J; Hasal P, Photocatalytic Degradation of Textile Dyes in aTiO<sub>2</sub>/UV System, *Chemical Engineering Transactions*, **2013**, 32, 79-84.
- [43] Leticia M Torres-Martinez; Isaias Jarez-Ramirez1; Juan S. Ramos-Garza1; Francisco Vazquez-Acosta1; Soo Wahn Lee2, Bi<sub>2</sub>MTaO<sub>7</sub> (M = Al, Fe, Ga, In) Photocatalyst For Organic Compounds Degradation Under UV And Visible Light *Wseas Transactions On Environment And Development*, **2010**, 6, 286-295.
- [44] Ortiz E; Solis H; Noreña L; Loera-Serna S, Degradation of Red Anthraquinone Dyes: Alizarin, Alizarin S and Alizarin Complexone by Ozonation, *International Journal of Environmental Science and Development*, **2017**, 8(4), 255-259
- [45] Nandre CV; Sawant CP, Photocatalytic Degradation of Alizarin Red-S by Fe-Co Nanoparticles Prepared By Chemical Coprecipitation Method, *Journal of Advances in Chemistry*, **2015**, 11(9), 3950-3958
- [46] Bharati DB; Bharati AV, Photocatalytic degradation of Alizarin Red dye under visible light using ZnO & CdO nanomaterial **2018**, 160, 371-379
- [47] Santhi K; Rani C; Karuppuchamy S, Degradation of Alizarin Red S dye using Ni doped WO<sub>3</sub>, Photocatalyst, *Journal of Materials Science: Materials in Electronics*, **2016**, 27(5), 5033-5038.
- [48] Loghman K; Salar Zohoori; Mohammad Esmail Y, Photocatalytic degradation of azo dyes in aqueous solutions under UV irradiation using nano-strontium titanate as the nanophotocatalyst, *Journal of Saudi Chemical Society*, **2014**, 18, 581–588.
- [49] Roopaei H; Zohdi AR; Abbasi Z; Bazrafkan M, Preparation of New Photocatalyst for Removal of Alizarin Red-S from Aqueous Solution, *Indian Journal of Science and Technology*, **2014**, 7(11), 1882–1887
- [50] Oussi D; Mokriani A; Esplugas S, *J Photochem. Photobiol. A: Chem.* **1997**, 1, 77.
- [51] Fox MA; Dulay MT, *Chem. Rev.*, **1993**, 93, 341.
- [52] Habibi MH; Hassanzadeh ; Zeini-Isfahani A, *Dyes Pigments*, **2006**, 69, 93.
- [53] Hihara T; Okada Y; Morita Z, *Dyes Pigments*, **2003**, 59, 25.
- [54] Viruthagiri G; Praveen P; Mugundan S; Anbuvaran M, Growth and Characterization of L-Histidine Doped Thiourea Single Crystals by Slow Evaporation Method, *Indian J. Advances in Chem. Science*, **2013**, 1, 193-200.

- 
- [55] Stankovich S; Dikin DA; Dommett GHB; Kohlhaas KM; Zimney EJ; Stach EA; Piner RD; Nguyen ST; Ruoff RS, Photocatalytic application of nano Graphene oxide material, *Nature*, **2006**, 442, 282-286.
- [56] Meng X; Zhang Z, “Synthesis, analysis and testing of BiOBr-Bi<sub>2</sub>WO<sub>6</sub> photocatalytic heterojunction semiconductors,” *International Journal of Photoenergy*, **2015**.